Tracking of Lines in Spherical Images via Sub-Riemannian Geodesics in $SO(3)$

Alexey Mashtakov[1], Remco Duits[2], Yuri Sachkov[1], Erik Bekkers[2], Ivan Beschastnyi[3]

Program Systems Institute of RAS[1]; Eindhoven University of Technology[2]; International School for Advanced Studies[3]

Introduction

In computer vision it is common to extract salient curves via minimal paths or geodesics [1]. These geodesics minimize a length functional based on a cost function on the image domain that has a low value at locations with high curve saliency. Inspired by [2], we proposed a computational framework [3] for tracking of lines in flat images via data-driven sub-Riemannian (SR) geodesics on the Euclidean motion group $SE(2)$.

In [3]: For given boundary conditions on a 2D plane to find a curve minimizing the compromise between length and curvature. External cost is included for adaptation to flat image.

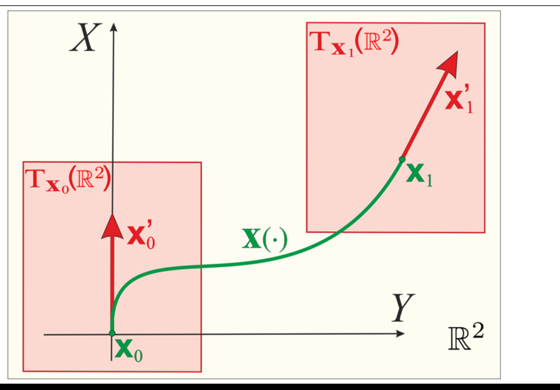

Now we extend the framework for tracking of lines in **spherical** images. This requires a SR manifold structure in the group $SO(3)$ of 3D-rotations acting transitively on the 2-sphere S^2.

Curve Minimization Problem $\mathbf{P_{curve}}$

$\mathbf{P_{curve}}$: For given boundary conditions on a 2D sphere (positions and velocities) to find a curve minimizing the functional compromising length and geodesic curvature. External cost in optimization functional is induced by spherical image.

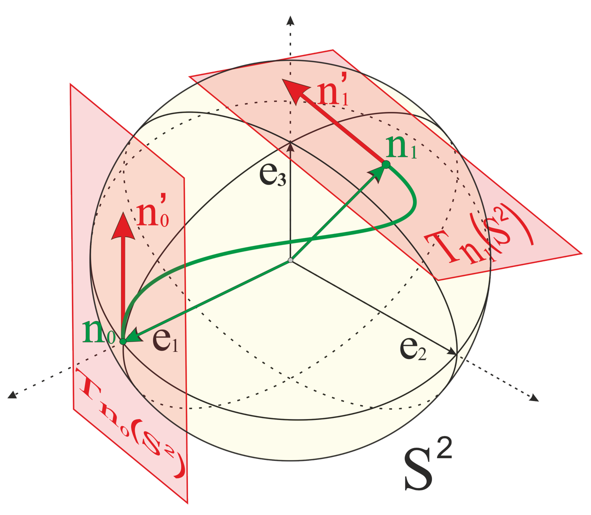

Given: constant $\xi > 0$,
$\mathbf{n}_0 \in S^2$, $\mathbf{n}'_0 \in T_{\mathbf{n}_0}(S^2)$,
$\mathbf{n}_1 \in S^2$, $\mathbf{n}'_1 \in T_{\mathbf{n}_1}(S^2)$,
external cost $\mathfrak{C} : S^2 \to \mathbb{R}^+$.

Find: $\mathbf{n}(\cdot) : [0, l] \to S^2$, s.t.
$\mathbf{n}(0) = \mathbf{n}_0$, $\mathbf{n}(l) = \mathbf{n}_1$,
$\mathbf{n}'(0) = \mathbf{n}'_0$, $\mathbf{n}'(l) = \mathbf{n}'_1$,
$\int_0^l \mathfrak{C}(\mathbf{n}(s))\sqrt{\xi^2 + k_g^2(s)}\,ds \to \min.$

3D Rotations Group SO(3)

Lie group $SO(3) \ni g \sim R(x, y, \theta) = R^{y}_{\mathbf{e}_3} R^{-x}_{\mathbf{e}_2} R^{\theta}_{\mathbf{e}_1}$,
where $R^{\varphi}_{\mathbf{a}}$ is a 3D rotation around axis $\mathbf{a} \in S^2$ by angle φ.

Basis left-invariant vector fields

$$\begin{aligned} \mathcal{A}_1|_g &= \cos\theta\,\partial_x|_g - \sec x \sin\theta\,\partial_y|_g + \tan x \sin\theta\,\partial_\theta|_g = (L_g)_*\,\partial_x|_e,\\ \mathcal{A}_2|_g &= \partial_\theta|_g = (L_g)_*\,\partial_\theta|_e,\\ \mathcal{A}_3|_g &= \sin\theta\,\partial_x|_g + \sec x \cos\theta\,\partial_y|_g - \tan x \cos\theta\,\partial_\theta|_g = (L_g)_*\,\partial_y|_e, \end{aligned}$$

where $(L_g)_*$ is push-forward of left multiplication $L_g h = gh$.

Basis left-invariant one forms $\langle \omega^i, \mathcal{A}_j \rangle = \delta^i_j$

Sub-Riemannian (SR) Problem $\mathbf{P_{mec}}$

Left-invariant distribution $\Delta = \text{span}\{\mathcal{A}_1, \mathcal{A}_2\} \subset T(SO(3))$

Metric tensor $\mathcal{G}|_g = \mathcal{C}^2(g)\left(\xi^2\omega^1 \otimes \omega^1 + \omega^2 \otimes \omega^2\right)|_g$ on Δ,

with external cost $\mathcal{C} : SO(3) \to [\delta, +\infty)$, $\delta > 0$, and $\xi > 0$.

SR-distance: Inf among Lipschitzian curves $\gamma : \mathbb{R} \to SO(3)$

$$d(e, g) = \inf\{\int_0^T \sqrt{\mathcal{G}|_{\gamma(t)}(\dot\gamma(t), \dot\gamma(t))}\,dt \mid \begin{array}{l}\gamma(0) = e,\\ \gamma(T) = g,\end{array} \dot\gamma(t) \in \Delta|_{\gamma(t)}\}.$$

SR-minimizers are solutions to the optimal control problem

$\mathbf{P_{mec}}$: $\gamma(0) = e, \quad \gamma(T) = g,$

$$\dot\gamma(t) = u_1(t)\,\mathcal{A}_1|_{\gamma(t)} + u_2(t)\,\mathcal{A}_2|_{\gamma(t)},$$

$$\int_0^T \mathcal{C}(\gamma(t))\sqrt{\xi^2 u_1(t)^2 + u_2(t)^2}\,dt \to \min.$$

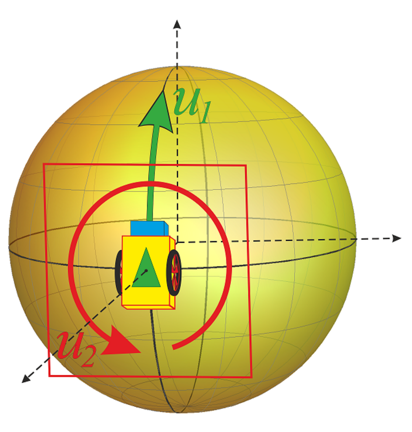

Optimal motion of Reeds-Shepp car on a sphere. Admissible motions forward/backward and rotations on a place are controlled by $(u_1, u_2) \in \mathbb{R}^2$.

Relation between $\mathbf{P_{mec}}$ and $\mathbf{P_{curve}}$

Theorem. Let $\gamma(t)$, $t \in [0, T]$, be a minimizer of $\mathbf{P_{mec}}$ parametrized by SR-arclength t. Let $u_1(t) > 0$ for all $t \in [0, T]$. Set $\mathbf{n}_0 = \mathbf{e}_1$, $\mathbf{n}'_0 = \mathbf{e}_3$, $\mathbf{n}_1 = \gamma(T)\,\mathbf{e}_1$, $\mathbf{n}'_1 = \gamma(T)\,\mathbf{e}_3$. Then for such boundary conditions $\mathbf{P_{curve}}$ has a minimizer $\mathbf{n}(s)$, along which $\mathbf{n}(s) = \gamma(t(s))\,\mathbf{e}_1$, $\quad u_1(t) = \frac{ds}{dt}(t)$, $\; u_2(t) = k_g(s(t))\frac{ds}{dt}(t)$,

and $t(s) = \int_0^s \mathfrak{C}(\mathbf{n}(\sigma))\sqrt{\xi^2 + k_g^2(\sigma)}\,d\sigma$.

Geodesics in Problem $\mathbf{P_{mec}}$ for $\mathcal{C} = 1$

By applying Pontryagin Maximum Principle we provide explicit formulas for SR geodesics. This allows us to describe the set of end points in $SO(3)$ reachable by geodesics whose spherical projections do not have cusps. We parameterize such "cuspless" SR geodesics by spherical arclength s and present new simpler formulas, which only involve a single elliptic integral.

Sub Riemannian Wave Front

End points of all the geodesics of the same length form SR wave front. When the wavefront intersect itself a geodesic is not longer a SR-minimizer (it loses optimality).

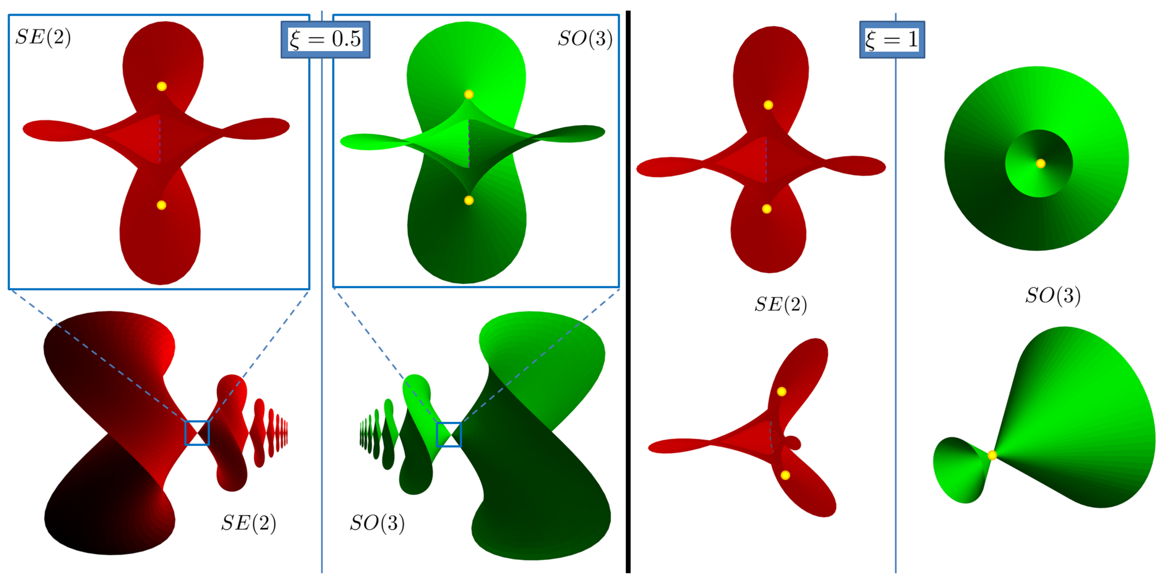

SR-minimizers in Problem $\mathbf{P_{mec}}$

Theorem. Let $\mathcal{W}(g)$ be a viscosity solution of eikonal system

$$\begin{cases} \sqrt{\frac{1}{\xi^2}\left(\mathcal{A}_1|_g(\mathcal{W})\right)^2 + \left(\mathcal{A}_2|_g(\mathcal{W})\right)^2} = \mathcal{C}(g), & \text{for } g \neq e,\\ \mathcal{W}(e) = 0. \end{cases}$$

Then $\mathcal{S}_t = \{g \in SO(3) \mid \mathcal{W}(g) = t\}$ are SR-spheres of radius t. SR-minimizer $\gamma(t)$ starting from e and ending at g is given by $\gamma(t) = \gamma_b(\mathcal{W}(g) - t)$, which is found by integration for $t \in [0, \mathcal{W}(g)]$

$$\dot\gamma_b(t) = -u_1(t)\,\mathcal{A}_1|_{\gamma_b(t)} - u_2(t)\,\mathcal{A}_2|_{\gamma_b(t)}, \qquad \gamma_b(0) = g,$$

where $u_1(t) = \dfrac{\mathcal{A}_1|_{\gamma_b(t)}(\mathcal{W})}{(\xi\,\mathcal{C}(\gamma_b(t)))^2}$ and $u_2(t) = \dfrac{\mathcal{A}_2|_{\gamma_b(t)}(\mathcal{W})}{(\mathcal{C}(\gamma_b(t)))^2}$.

Similarly to [4] we provide SR Fast Marching (SR-FM) method.

Validation for Uniform Cost $\mathcal{C} = 1$

Comparison of the exact SR-geodesics and the SR-minimizers computed numerically shows an accurate result of SR-FM.

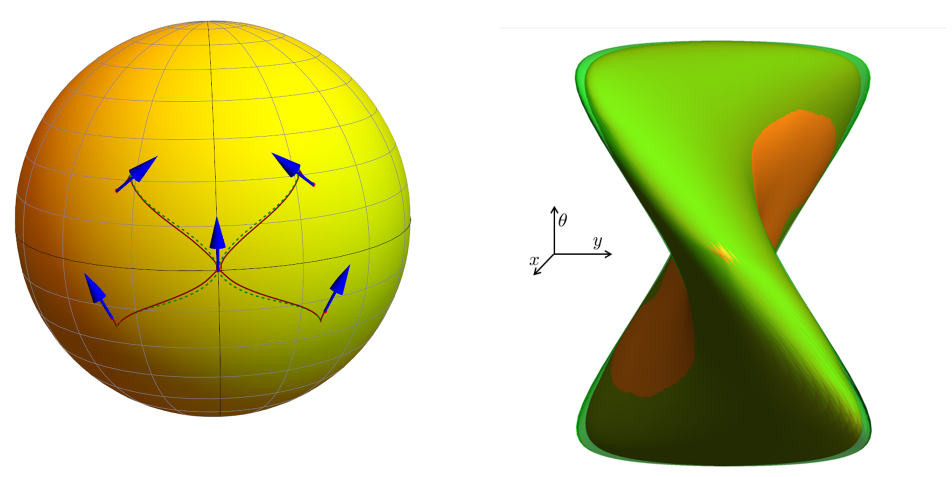

Existence of nonoptimal cuspless geodesics (contra $SE(2)$).

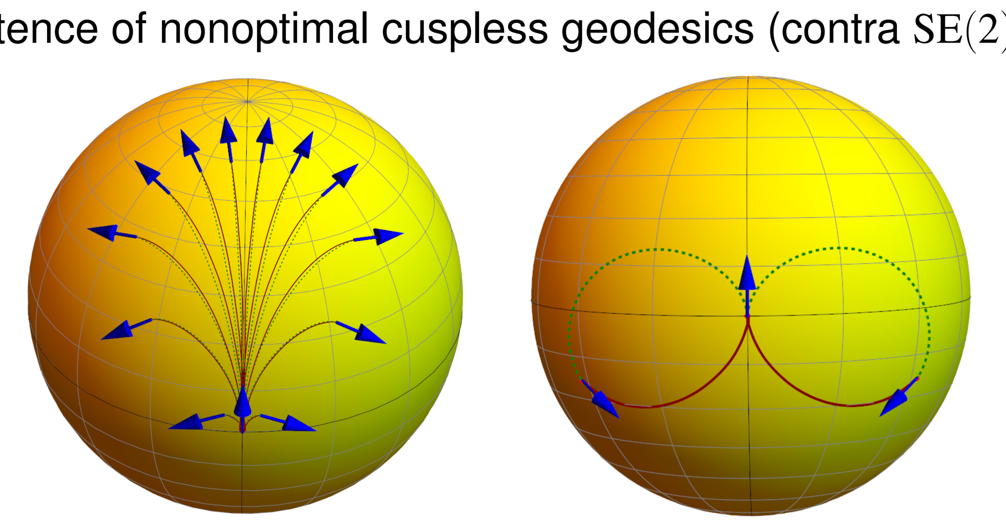

Application in Retinal Imaging

The retinal vasculature enables non-invasive observation of the human circulatory system. A variety of eye-related and systematic diseases affect the vasculature and may cause functional or geometric changes. Vascular tree must be detected for automated quantification of these defects.

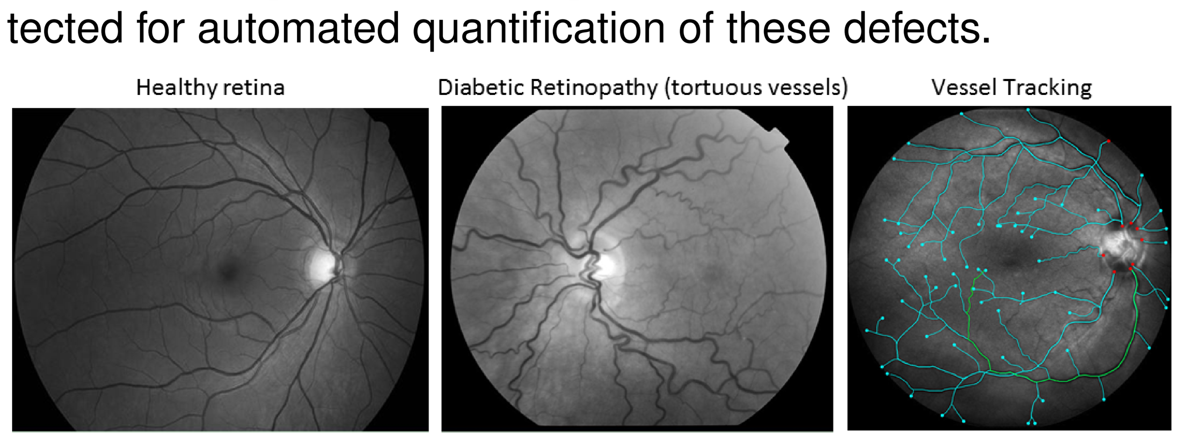

Spherical Images of Retina

Optical retinal images are mostly acquired by flat cameras, and as a result distortion appears. Such distortion comes from the central projection of the physical retinal surface to the image plane. It can lead to questionable geometrical features (e.g. vessel curvature) that are used as biomarkers [5] for different diseases. We show that the distortion can play a significant role in the quantitative analysis of the vascular structure.

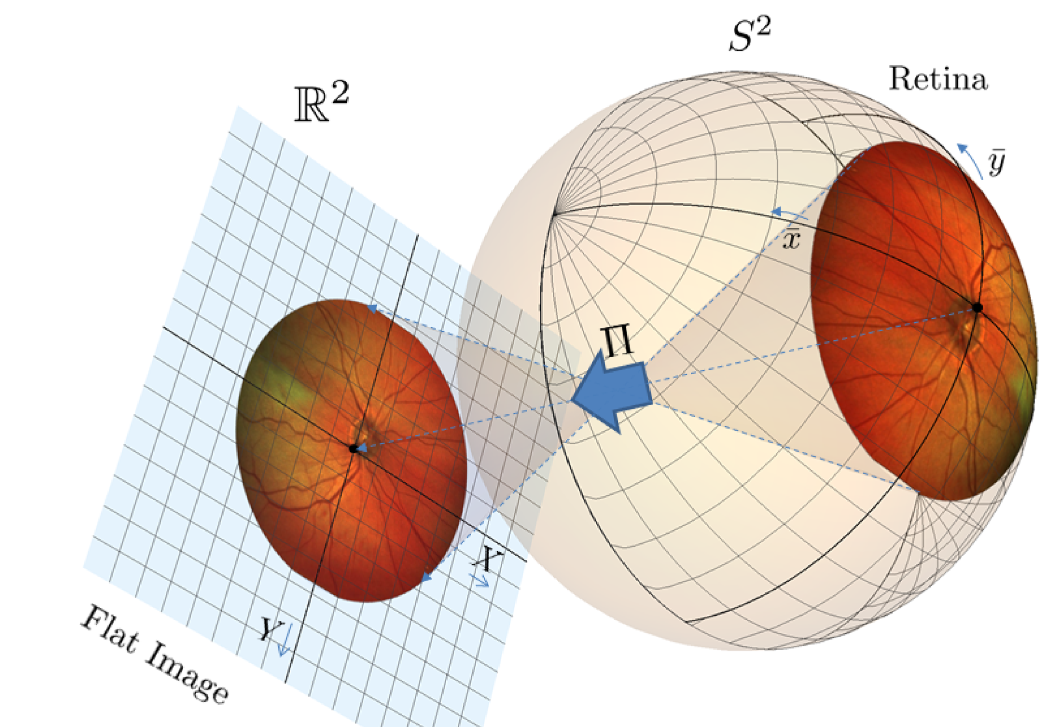

Vessel Tracking

Experiment in a spherical image of the retina shows that $SO(3)$ geodesics are less eager to take short cuts than $SE(2)$ geodesics [3] in vessel tracking. The results are stable w.r.t. choice of distance $1 < \eta < 2$ from the camera to the eye ball.

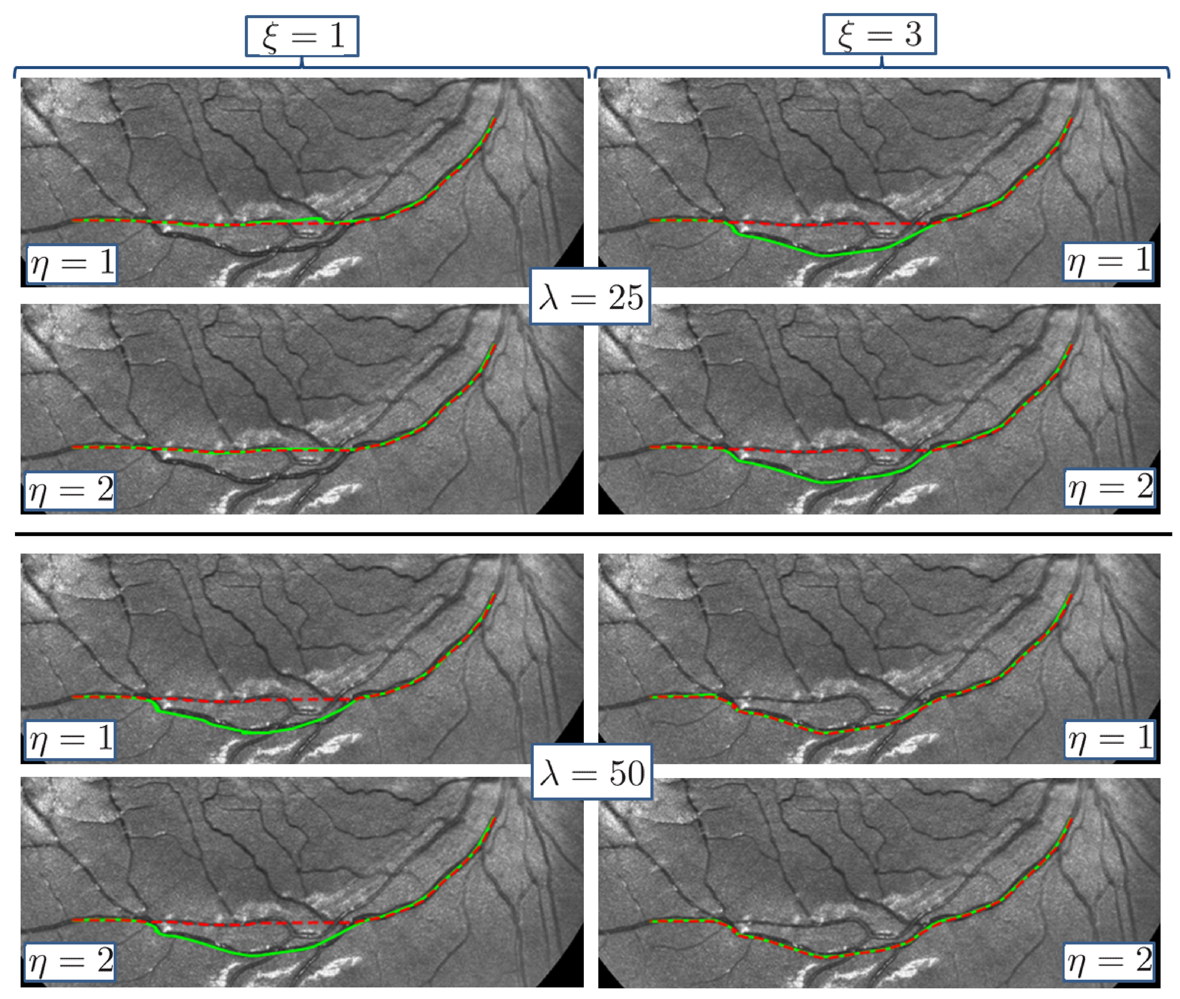

Vessel Curvature Measurement

The effect of considering geodesic curvature $\kappa_g^{SO(3)}$ in object coordinates on S^2 rather than planar curvature $\kappa^{SO(3)}$ in photo coordinates on projection on $\mathbb{R}^2$ is visible. A bigger difference comes from using $SO(3)$ than $SE(2)$ SR-geometry.

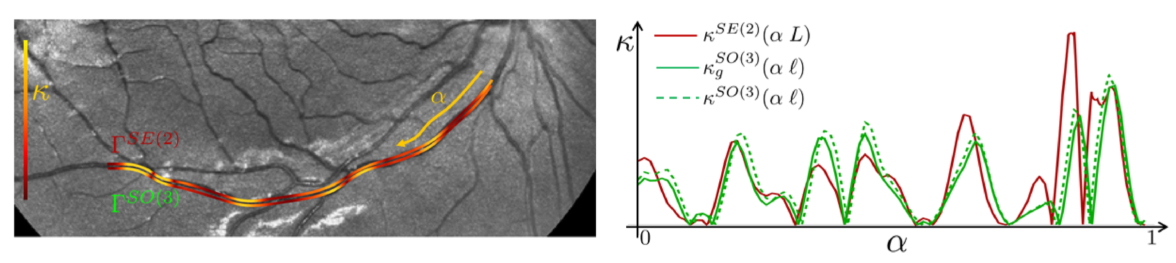

Results

We present new explicit formulas for SR geodesics in $SO(3)$ with cuspless spherical projection, simpler than for general geodesics. Furthermore we propose a PDE theory, that allows us to numerically compute the SR-minimizers for general external cost and general $\xi > 0$. Our numerical solution was verified by comparison with exact geodesics for $\mathcal{C} = 1$.

We use these results in a vessel tracking algorithm in spherical images of the retina, without central projection distortion. Experiments show considerable difference in vessel curvature measurement via $SE(2)$ geodesics and $SO(3)$ geodesics.

As in retinal imaging applications curvature is considered as a relevant biomarker for detection of diabetic retinopathy and other systemic diseases, the data-driven SR geodesic model in $SO(3)$ is a relevant extension of our model [3] in $SE(2)$.

Bibliography

[S] Mashtakov A., Duits R., Sachkov Yu., Bekkers E., Beschastnyi I. *Tracking of Lines in Spherical Images via Sub-Riemannian Geodesics in $SO(3)$*, arXiv, 2016. **[1]** G. Peyré, M. Péchaud, R. Keriven, L.D. Cohen, *Geodesic methods in computer vision and graphics*, FTCCGV, 2010. **[2]** G. Citti, A. Sarti, *A cortical based model of perceptual completion in the roto-translation space*, JMIV, 2006. **[3]** E.J. Bekkers, R. Duits, A. Mashtakov and G.R. Sanguinetti, *A PDE Approach to Data-driven Sub-Riemannian Geodesics in $SE(2)$*, SIIMS, 2015. **[4]** G. Sanguinetti, R. Duits, E. Bekkers, M. Janssen, A. Mashtakov, J-M. Mirebeau, *Sub-Riemannian Fast Marching in $SE(2)$*, CIARP, 2015. **[5]** Bekkers E., Zhang J., Duits R., ter Haar Romeny B., *Curvature based biomarkers for diabetic retinopathy via exponential curve fits in SE(2)*, MICCAI 2015. **[6]** Duits R., Boscain U., Rossi F., Sachkov Y. L., *Association Fields via Cuspless Sub-Riemannian Geodesics in $SE(2)$*, JMIV, 2014. **[7]** U. Boscain, F. Rossi, *Projective Reed-Shepp Car on S^2*, ESAIM COCV, 2009. **[8]** V.Berestovskii, I. Zubareva, *Sub-Riemannian distance in the Lie groups $SU(2)$ and $SO(3)$*, SAM, 2016. **[9]** Mashtakov A.P., Ardentov A.A., Sachkov Y.L., *Parallel Algorithm and Software for Image Inpainting via Sub-Riemannian Minimizers on the Group of Rototranslations*, NMTMA, 2013.